

Adaptive Cell-Centered Finite Volume Method

Christoph Erath, Stefan Funken and Dirk Praetorius

Preprint Series: 2008-01



Fakultät für Mathematik und Wirtschaftswissenschaften
UNIVERSITÄT ULM

Adaptive Cell-Centered Finite Volume Method

Christoph Erath* — Stefan Funken* — Dirk Praetorius**

* University of Ulm, Institute for Numerical Mathematics
Helmholtzstraße 18
D-89069 Ulm, Germany
{Christoph.Erath,Stefan.Funken}@uni-ulm.de

** Vienna University of Technology, Institute for Analysis and Scientific Computing
Wiedner Hauptstraße 8-10
A-1040 Vienna, Austria
Dirk.Praetorius@tuwien.ac.at

ABSTRACT. In our talk, we propose an adaptive mesh-refining strategy for the cell-centered FVM based on some a posteriori error control for the quantity $\|\nabla_{\mathcal{T}}(u - \mathcal{I}u_h)\|_{L^2}$. Here, $u_h \in \mathcal{P}^0(\mathcal{T})$ denotes the FVM approximation of u and \mathcal{I} is a certain interpolation operator. As model example serves the Laplace equation with mixed boundary conditions, where our contributions extend a result of [NIC05]. Moreover, this approach allows the coupling of finite volume schemes with the boundary element method, which is a new and fruitful combination of the shown ideas in [CAR99a, CAR99b] and given below.

KEYWORDS: finite volume method, cell-centered method, diamond path, a posteriori error estimate, adaptive algorithm

1. Introduction and Elliptic Model Problem

We consider a bounded and connected domain $\Omega \subset \mathbb{R}^2$ with Lipschitz boundary $\Gamma := \partial\Omega$, which is divided into a closed Dirichlet boundary $\Gamma_D \subseteq \Gamma$ with positive surface measure and a Neumann boundary $\Gamma_N := \Gamma \setminus \Gamma_D$. We then consider the elliptic boundary value problem

$$\begin{aligned} -\Delta u &= f && \text{in } \Omega, \\ u &= u_D && \text{on } \Gamma_D \quad \text{and} \quad \partial u / \partial \mathbf{n} = g && \text{on } \Gamma_N. \end{aligned} \tag{1.1}$$

Here, $f \in L^2(\Omega)$, $u_D \in H^1(\Gamma_D)$, and $g \in L^2(\Gamma_N)$ are given data, and $L^2(\cdot)$ and $H^1(\cdot)$ denote the standard Lebesgue- and Sobolev-spaces equipped with the usual norms $\|\cdot\|_{L^2(\cdot)}$ and $\|\cdot\|_{H^1(\cdot)}$. We aim to approximate the unique weak solution

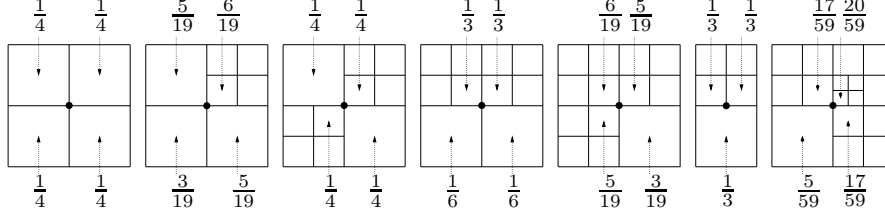


Figure 2.1. The weights ψ_T for an almost regular mesh of squares.

$u \in H^1(\Omega)$ by a postprocessed finite volume scheme. Throughout, \mathcal{T} denotes a certain triangulation of Ω , where \mathcal{N} and \mathcal{E} are the corresponding sets of nodes and edges, respectively. The set of nodes (edges) on the Dirichlet resp. Neumann boundary are \mathcal{N}_D resp. \mathcal{N}_N (\mathcal{E}_D resp. \mathcal{E}_N). For brevity, we assume that the elements $T \in \mathcal{T}$ are non-degenerate rectangles and refer to [ERA07] for triangular elements. For $T \in \mathcal{T}$, $h_T := \text{diam}(T)$ denotes the Euclidean diameter and for an edge $E \in \mathcal{E}$, we denote by h_E its length. We say that the triangulation \mathcal{T} is *almost regular*, if

- (i) the mixed boundary conditions are resolved, i.e. each edge $E \in \mathcal{E}$ with $E \cap \Gamma \neq \emptyset$ satisfies either $E \subseteq \bar{\Gamma}_D$ or $E \subseteq \bar{\Gamma}_N$.
- (ii) the intersection $T_1 \cap T_2$ of two elements $T_1, T_2 \in \mathcal{T}$ with $T_1 \neq T_2$ is either empty or a node or an edge.
- (iii) the edge $E \in \mathcal{E}$ contains an interior (i.e. hanging) node, there are two edges $E_1, E_2 \in \mathcal{E}$ with $E = E_1 \cup E_2$, cf. figure 2.1 for examples.

A node $a \in \mathcal{N} \setminus (\mathcal{N}_D \cup \mathcal{N}_N)$ is a hanging node provided that there are elements $T_1, T_2 \in \mathcal{T}$ such that $a \in T_1 \cap T_2$ is a node of T_1 but not of T_2 . Let \mathcal{N}_H be the set of all hanging nodes.

2. Cell-Centered Finite Volume Method

We integrate the differential equation (1.1) over a control volume $T \in \mathcal{T}$ and use the Gauss divergence theorem to obtain, with \mathcal{E}_T the set of edges of T ,

$$\int_T f \, dx = - \int_{\partial T} \frac{\partial u}{\partial \mathbf{n}_T} \, ds = - \sum_{E \in \mathcal{E}_T} \Phi_{T,E}(u) \, ds \quad \text{for all } T \in \mathcal{T}.$$

Here, $\Phi_{T,E}(u) = \int_E \partial u / \partial \mathbf{n}_{T,E} \, ds$ is the diffusive flux and $\mathbf{n}_{T,E}$ is the outer normal vector of T on E . Let $u_h \in \mathcal{P}^0(\mathcal{T})$ be a piecewise constant approximation of u , namely $u_T := u_h|_T \approx u(x_T)$, where x_T denotes the center of an element $T \in \mathcal{T}$. For the cell-centered finite volume method, u_h is computed by replacing the diffusion flux $\Phi_{T,E}(u)$ by a discrete diffusion flux $F_{T,E}(u_h)$. First, $\Phi_{T,E}(u) = \int_E g \, ds$ is known for a Neumann edge $E \in \mathcal{E}_N$. One therefore defines

$$F_{T,E}(u_h) := \Phi_{T,E}(u_h) = \int_E g \, ds \quad \text{for } E \in \mathcal{E}_N.$$

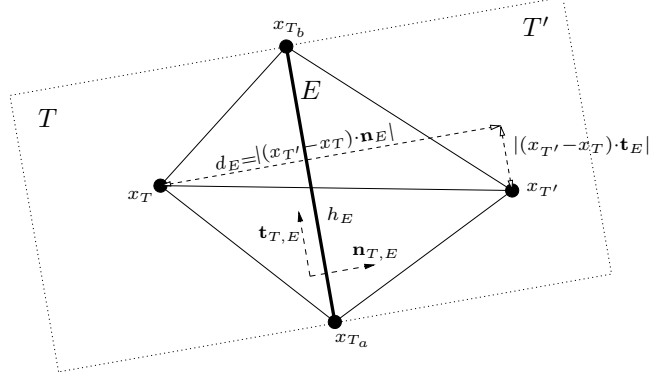


Figure 2.2. Notation for the diamond path.

Second, for a non-elementary edge with $E = E_1 \cup E_2 \in \mathcal{E}$ and $E_1, E_2 \in \mathcal{E}_E$, where \mathcal{E}_E denotes the set of elementary edges (i.e. neither E_1 nor E_2 contain an interior node), there holds $\Phi_{T,E}(u) = \Phi_{T,E_1}(u) + \Phi_{T,E_2}(u)$, which leads to the definition

$$F_{T,E}(u_h) := F_{T,E_1}(u_h) + F_{T,E_2}(u_h) \quad \text{for } E = E_1 \cup E_2 \in \mathcal{E} \text{ with } E_1, E_2 \in \mathcal{E}_E.$$

Finally, it remains to define $F_{T,E}(u_h)$ for elementary and Dirichlet edges $E \in \mathcal{E}_E \cup \mathcal{E}_D$. This is done by the *diamond path* method in the following way: For each node $a \in \mathcal{N}$, we define

$$u_a = \begin{cases} \sum_{T \in \tilde{\omega}_a} \psi_T(a) u_T, & \text{for all } a \in \mathcal{N} \setminus (\mathcal{N}_D \cup \mathcal{N}_N), \\ u_D(a), & \text{for all } a \in \mathcal{N}_D, \\ \bar{u}_a + \bar{g}_a, & \text{for all } a \in \mathcal{N}_N, \end{cases} \quad (2.1)$$

with certain weights $\{\psi_T(a) \mid T \in \mathcal{T}, a \in \mathcal{N}_T\}$ for each element of the patch $\tilde{\omega}_a := \{T \in \mathcal{T} \mid a \in \partial T\}$. Here, \mathcal{N}_T denotes the set of nodes of T . For details on the computation of the weights, the reader is referred to [COU00]. Figure 2.1 gives the precise values for almost regular triangulations of squares. Details on the computation of \bar{u}_a and \bar{g}_a are found in [ERA07]. For an elementary edge $E \in \mathcal{E}_E$, let x_{T_a} and x_{T_b} be the starting and end point of $E \in \mathcal{E}_E \cup \mathcal{E}_D$ and $T, T' \in \mathcal{T}$ the unique elements with $E = T \cap T'$, cf. Figure 2.2. Then,

$$F_{T,E}(u_h) := h_E \left(\frac{u_{T'} - u_T}{d_E} - \alpha_E \frac{u_{T_b} - u_{T_a}}{h_E} \right) \quad (2.2)$$

with $\alpha_E = \frac{(x_{T'} - x_T) \cdot \mathbf{t}_{T,E}}{(x_{T'} - x_T) \cdot \mathbf{n}_{T,E}}, \quad d_E = (x_{T'} - x_T) \cdot \mathbf{n}_{T,E}.$

Here, the additional unknowns u_{T_b} and u_{T_a} are located at the nodes x_{T_b} and x_{T_a} and are computed by (2.1). Finally, the tangential vector $\mathbf{t}_{T,E}$ is chosen orthogonal to

$\mathbf{n}_{T,E}$ in mathematical positive sense. For a boundary edge $E \in \mathcal{E}_D$, we compute $F_{T,E}(u_h)$ by (2.2), where $x_{T'}$ is now replaced by the midpoint x_{E_m} of E and u_{T_E} becomes $u_D(x_{E_m})$. Altogether, the discrete problem reads: Find $u_h \in \mathcal{P}^0(\mathcal{T})$ such that

$$-\sum_{E \in \mathcal{E}_T} F_{T,E}(u_h) = \int_T f \, dx, \quad \text{for all } T \in \mathcal{T}.$$

Note, that the conservativity of the continuous flux $\Phi_{T,E}(u) = -\Phi_{T',E}(u)$ also holds for the discrete flux $F_{T,E}(u_h) = -F_{T',E}(u_h)$.

REMARK. — We stress, that even for an admissible triangular mesh \mathcal{T} in the sense of [EYM00, Definition 9.1], local mesh-refinement is nontrivial, since admissibility necessarily implies that all angles are strictly less than $\pi/2$. For rectangular meshes, local mesh-refinement cannot avoid hanging nodes and thus contradicts the admissibility condition.

3. A Posteriori Error Estimate

For non-degenerate rectangular element $T = \text{conv}\{a_1, a_2, a_3, a_4\} \subset \mathbb{R}^2$ with edges $E_j = \text{conv}\{a_j, a_{j+1}\}$ and $a_5 := a_1$, a Morley-type element $(T, \mathcal{P}_T, \Sigma_T)$ is given by $\mathcal{P}_T = \mathcal{P}_2 \oplus \text{span}\{x^3 - 3xy^2, y^3 - 3yx^2\}$ and $\Sigma_T = (S_1, \dots, S_8)$, where

$$S_j(p) = p(a_j), \quad S_{j+4}(p) = \int_{E_j} \frac{\partial p}{\partial \mathbf{n}_{T,E_j}} \, ds \quad \text{for } j = 1, \dots, 4 \quad (p \in \mathcal{P}_T),$$

cf. [NIC05, Section 4.2]. Then, $(T, \mathcal{P}_T, \Sigma_T)$ is a nonconforming finite element. The Morley interpolant $\mathcal{I}u_h$ is now defined \mathcal{T} -elementwise by (3.1)–(3.4). The definition of which is an extension of the definition in [NIC05, Section 5] to the case of hanging nodes and mixed boundary conditions. For each free node $a \in \mathcal{N}_T \cap (\mathcal{N} \setminus (\mathcal{N}_D \cup \mathcal{N}_N \cup \mathcal{N}_H))$, we enforce

$$(\mathcal{I}u_h)|_T(a) = \sum_{T_a \in \tilde{\omega}_a} \psi_{T_a}(a) u_h|_{T_a}. \quad (3.1)$$

For each boundary node, the value $\mathcal{I}u_h(a)$ is prescribed by

$$(\mathcal{I}u_h)|_T(a) = \begin{cases} u_D(a) & \text{for } a \in \mathcal{N}_T \cap \mathcal{N}_D, \\ \bar{u}_a + \bar{g}_a & \text{for } a \in \mathcal{N}_T \cap \mathcal{N}_N. \end{cases} \quad (3.2)$$

For each hanging node $a \in \mathcal{N}_T \cap \mathcal{N}_H$, there holds

$$(\mathcal{I}u_h)|_T(a) = (\mathcal{I}u_h)|_{T_a}(a), \quad (3.3)$$

where $T_a \in \mathcal{T}$ is the unique element with $a \in \text{int}(E)$ for some (non-elementary) edge $E \in \mathcal{E}_{T_a}$. Finally, for each edge $E \in \mathcal{E}_T$ holds

$$\int_E \frac{\partial(\mathcal{I}u_h)|_T}{\partial \mathbf{n}_{T,E}} \, ds = F_{T,E}(u_h). \quad (3.4)$$

We stress, that the Morley interpolant $\mathcal{I}u_h$ is uniquely defined by (3.1)–(3.4). Moreover, the definition ensures the following orthogonality properties, which are essential for the analysis of the proposed error estimator. The residual $R := f + \Delta(\mathcal{I}u_h)$ is L^2 -orthogonal to $\mathcal{P}^0(\mathcal{T})$, i.e.

$$\int_T (f + \Delta(\mathcal{I}u_h)) dx = 0 \quad \text{for all } T \in \mathcal{T}.$$

In particular, $R = f - f_T$, where f_T denotes the T -piecewise integral mean, i.e. $f_T|_T := |T|^{-1} \int_T f dx$. For boundary edges hold

$$\int_E \frac{\partial(u - \mathcal{I}u_h)}{\partial \mathbf{t}_{T,E}} ds = 0 \quad (E \in \mathcal{E}_D) \quad \text{resp.} \quad \int_E \frac{\partial(u - \mathcal{I}u_h)}{\partial \mathbf{n}_{T,E}} ds = 0 \quad (E \in \mathcal{E}_N)$$

and for the interior edges hold

$$\int_E \left[\frac{\partial(\mathcal{I}u_h)}{\partial \mathbf{n}_{T,E}} \right] ds = 0 \quad (E \in \mathcal{E}_0) \quad \text{resp.} \quad \int_E \left[\frac{\partial(\mathcal{I}u_h)}{\partial \mathbf{t}_{T,E}} \right] ds = 0 \quad (E \in \mathcal{E}_E).$$

where \mathcal{E}_0 denotes the set of all interior edges which are not part of a non-elementary edge. Here, the jump over $E \in \mathcal{E}_E$ reads

$$[\partial(\mathcal{I}u_h)/\partial \mathbf{n}_{T,E}] = \partial(\mathcal{I}u_h)/\partial \mathbf{n}_{T,E} + \partial(\mathcal{I}u_h)/\partial \mathbf{n}_{T',E},$$

where $T, T' \in \mathcal{T}$ and $E = T \cap T'$. Note that $\mathbf{n}_{T,E} = -\mathbf{n}_{T',E}$ so that the sum in the definition is in fact a difference. For each non-elementary edge $E = E_1 \cup E_2 \in \mathcal{E}$ with $E_1, E_2 \in \mathcal{E}_E$, we define the jump

$$[\partial(\mathcal{I}u_h)/\partial \mathbf{n}_{T,E}]_E(x) := [\partial(\mathcal{I}u_h)/\partial \mathbf{n}_{T,E}]_{E_i}(x) \quad \text{for all } x \in E_i, \quad i = 1, 2.$$

The tangential jump $[\partial(\mathcal{I}u_h)/\partial \mathbf{t}_{T,E}]$ is defined analogously. For each element $T \in \mathcal{T}$, we define the refinement indicator

$$\begin{aligned} \eta_T^2 := & h_T^2 \|f - f_T\|_{L^2(T)}^2 + \sum_{E \in \mathcal{E}_T \setminus (\mathcal{E}_D \cup \mathcal{E}_N)} h_E \|\nabla_T(\mathcal{I}u_h)\|_{L^2(E)}^2 \\ & + \sum_{E \in \mathcal{E}_T \cap \mathcal{E}_N} h_E \left\| \frac{\partial(u - \mathcal{I}u_h)}{\partial \mathbf{n}_{T,E}} \right\|_{L^2(E)}^2 + \sum_{E \in \mathcal{E}_T \cap \mathcal{E}_D} h_E \left\| \frac{\partial(u - \mathcal{I}u_h)}{\partial \mathbf{t}_{T,E}} \right\|_{L^2(E)}^2. \end{aligned} \quad (3.5)$$

With techniques known from the finite element method [AIN00], one proves reliability

$$C_{\text{rel}}^{-1} \|\nabla_T(u - \mathcal{I}u_h)\|_{L^2(\Omega)} \leq \eta := \left(\sum_{T \in \mathcal{T}} \eta_T^2 \right)^{1/2}. \quad (3.6)$$

As for non-conforming FEM the proof employs a Helmholtz decomposition. The Galerkin orthogonality is replaced by the orthogonality properties of $\mathcal{I}u_h$ stated before. The converse inequality holds even T -elementwise, namely for all $T \in \mathcal{T}$

$$C_{\text{loc}}^{-1} \eta_T \leq \left(\|\nabla_T(u - \mathcal{I}u_h)\|_{L^2(\omega_T)}^2 + h_T^2 \|f - f_T\|_{L^2(\omega_T)}^2 \right)^{1/2}, \quad (3.7)$$

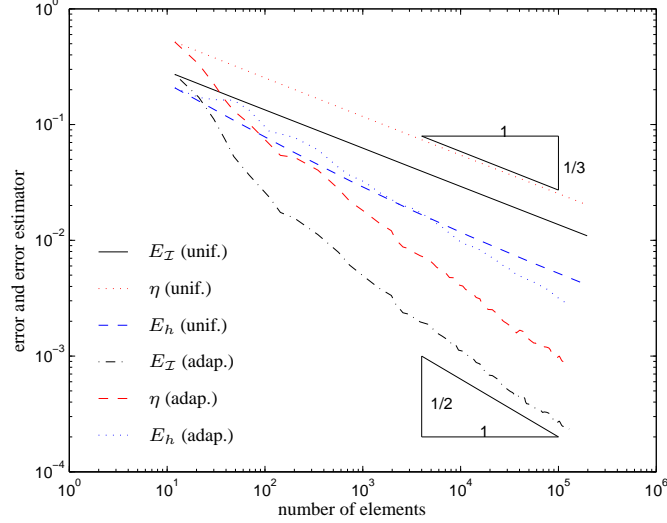


Figure 4.1. Errors $E_{\mathcal{T}}$ and E_h , estimator η in problem (1.1) for unif. and adap. ref.

where the involved patch reads $\omega_T := \bigcup \{T' \in \mathcal{T} \mid T \cap T' \neq \emptyset\}$. This estimate follows by usual technics and the use of appropriate bubble functions. In particular we obtain efficiency of η up to oscillation terms,

$$C_{\text{eff}}^{-1} \eta \leq \|\nabla_{\mathcal{T}}(u - \mathcal{I}u_h)\|_{L^2(\Omega)}^2 + h^2 \|f - f_{\mathcal{T}}\|_{L^2(\Omega)}^2. \quad (3.8)$$

The constants $C_{\text{rel}}, C_{\text{loc}}, C_{\text{eff}} > 0$ only depend on the shape of the elements in \mathcal{T} . We refer to [ERA07] for the detailed proofs of the estimates (3.6)–(3.8).

4. Numerical Experiments

We consider the Laplace problem (1.1) on the L-shaped domain $\Omega = (-1, 1)^2 \setminus ([0, 1] \times [-1, 0])$. The given exact solution is the harmonic function $u(x, y) = \Im((x + iy)^{2/3})$ and reads in polar coordinates

$$u(x, y) = r^{2/3} \sin(2\varphi/3) \quad \text{with} \quad (x, y) = r(\cos \varphi, \sin \varphi).$$

Note that u has a generic singularity at the reentrant corner $(0, 0)$. For the numerical computation, we prescribe the exact Neumann and Dirichlet data, where $\Gamma_D = \Gamma \setminus \Gamma_N$ and $\Gamma_N := \{0\} \times (-1, 0) \cup (0, 1) \times \{0\}$. Note that Γ_N includes the reentrant corner, where the normal derivative $\partial u / \partial \mathbf{n}$ is singular. We compute the energy error $E_h :=$

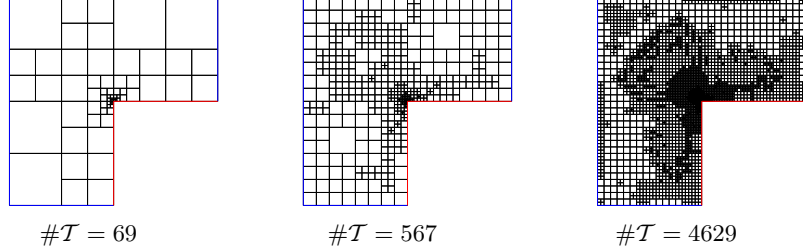


Figure 4.2. *Adaptively generated meshes in problem (1.1).*

$(\|u - u_h\|_{L^2(\Omega)}^2 + |u_{\mathcal{T}} - u_h|_{1,h}^2)^{1/2}$, with $u_{\mathcal{T}} \in \mathcal{P}^0(\mathcal{T})$ the \mathcal{T} -piecewise integral mean of u , and where the discrete H^1 -seminorm is defined by

$$|v_h|_{1,h} = \left(\sum_{E \in \mathcal{E}_E \cup \mathcal{E}_D} \left| (v_{T'} - v_T) / d_E \right|^2 h_E d_E \right)^{1/2}$$

for any $v_h \in \mathcal{P}^0(\mathcal{T})$. According to [COU00], the diamond path method satisfies $E_h = \mathcal{O}(N^{-1/2})$ with $N = |\mathcal{T}|$ provided that $u \in H^2(\Omega)$. Moreover, we compute the Morley error $E_{\mathcal{T}} = \|\nabla_{\mathcal{T}}(u - \mathcal{I}u_h)\|_{L^2(\Omega)}$ and the corresponding error estimator η . All computations are done in MATLAB in the spirit of [ALB99, ERA08]. We employ an adaptive mesh-refining algorithm, which is steered by the local refinement indicators η_T from (3.5): An element $T_j \in \mathcal{T}$ is marked for refinement provided $\eta_{T_j} \geq \theta \max\{\eta_{T_1}, \dots, \eta_{T_N}\}$, where we use $\theta = 0$ for uniform and $\theta = 0.5$ for adaptive mesh-refinement, respectively. The numerical outcome is plotted in Figure 4.1 over the number N of elements. For uniform mesh-refinement, the energy error E_h converges with a suboptimal order which appears to be slightly better than $\mathcal{O}(N^{-1/3})$. The proposed adaptive strategy regains the optimal order of convergence $\mathcal{O}(N^{-1/2})$. As can be expected from the finite element method, the Morley error $E_{\mathcal{T}}$ decreases like $\mathcal{O}(N^{-1/3})$ for uniform mesh-refinement. The adaptive algorithm leads to an improved order of convergence $\mathcal{O}(N^{-1/2})$. As predicted by theory, the error estimator η is observed to be reliable and efficient.

5. Outlook

The finite volume method is a well adapted method for the discretization of various convection dominated partial differential equations. It is very popular in the engineering community (fluid mechanics) because of its conservative properties. This method is contrary to the boundary element method (BEM), which can be applied to the most important linear and homogeneous partial differential equations with constant coefficients also in unbounded domains. The coupling of FVM and BEM combines the advantages of both methods, e.g. in problems where stationary diffusive heat and convection in different media are coupled. While convection would be modelled by the

finite volume method, diffusive heat (in a possibly unbounded domain) is solved using the boundary element method.

First numerical examples show the efficiency of the symmetric coupling of FVM and BEM, where we used the results given here for the FVM and results from [CAR99a, CAR99b] to develop a stable discretization. The resulting system of linear equations is now a 4×4 block-system instead of a 3×3 system for the FEM^{NC}-BEM coupling.

The coupling of FVM and BEM involves two further continuous ansatz functions on the interface to link the discontinuous displacement field to necessarily continuous boundary ansatz functions on the boundary. Quasi-optimal a priori error estimates and sharp a posteriori error estimates are almost established which justify adaptive mesh-refining algorithms. Numerical experiments show the adaptive coupling as an efficient tool for the numerical treatment of transmission problems.

6. References

- [AIN00] M. AINSWORTH, J.T. ODEN: *A posteriori error estimation in finite element analysis*, John Wiley & Sons, 2000.
- [ALB99] J. ALBERTY, C. CARSTENSEN, S.A. FUNKEN: *Remarks around 50 lines of Matlab: short finite element implementation*, Num. Alg., 20:117–137, 1999.
- [CAR99a] C. CARSTENSEN, S. A. FUNKEN: *Coupling of nonconforming finite elements and boundary elements I: A priori estimates*, Computing, 62:229–241, 1999.
- [CAR99b] C. CARSTENSEN, S. A. FUNKEN: *Coupling of nonconforming finite elements and boundary elements II: A posteriori estimates and adaptive mesh-refinement*, Computing, 62:243–259, 1999.
- [CIA78] P.G. CIARLET: *The finite element method for elliptic problems*, North-Holland, Amsterdam, 1978.
- [COU00] Y. COUDIÉRE, P. VILLEDIEU: *Convergence rate of a finite volume scheme for the linear convection-diffusion equation on locally refined meshes*, ESAIM: M2AN, 34(6):1123–1149, 2000.
- [ERA08] C. ERATH, S. FUNKEN, D. PRAETORIUS: *Matlab implementation of the finite volume method, part II: The cell centered FVM*, in preparation, 2008.
- [ERA07] C. ERATH, D. PRAETORIUS: *A posteriori error estimate and adaptive mesh-refinement for the cell-centered finite volume method for elliptic boundary value problems*, submitted 2007.
- [EYM00] R. EYMARD, T. GALLOUËT, R. HERBIN: *Finite volume methods*, Handbook of Numerical Analysis, Volume 7. Elsevier Science B.V., first edition, 1999.
- [NIC05] S. NICAISE: *A posteriori error estimations of some cell-centered finite volume methods*, SIAM J. Numer. Anal., 43(04):1481–1503, 2005.

